Integrated Active Fault-Tolerant Control Using IMM Approach

YOUMIN ZHANG, Member, IEEE
JIN JIANG, Senior Member, IEEE
The University of Western Ontario

An integrated fault detection, diagnosis, and reconfigurable control scheme based on interacting multiple model (IMM) approach is proposed. Fault detection and diagnosis (FDD) is carried out using an IMM estimator. An eigenstructure assignment (EA) technique is used for reconfigurable feedback control law design. To achieve steady-state tracking, reconfigurable feedforward controllers are also synthesized using input weighting approach. The developed scheme can deal with not only actuator and sensor faults, but also failures in system components. To achieve fast and reliable fault detection, diagnosis, and controller reconfiguration, new fault diagnosis and controller reconfiguration mechanisms have been developed by a suitable combination of the information provided by the mode *probabilities* from the IMM algorithm and an index related to the closed-loop system performance. The proposed approach is evaluated using an aircraft example, and excellent results have been obtained.

Manuscript received December 20, 1999; revised and resubmitted December 5, 2000; released for publication July 2, 2001.

IEEE Log No. T-AES/37/4/10988.

Refereeing of this contribution was handled by A. Ray.

This work was supported by the Natural Sciences and Engineering Research Council of Canada.

Authors' address: Department of Electrical and Computer Engineering, The University of Western Ontario, London, Ontario N6A 5B9, Canada, E-mail: ({ymzhang, jjiang}@uwo.ca).

0018-9251/01/$17.00

I. INTRODUCTION

The growing demand for reliability, maintainability, and survivability in safety critical systems has drawn significant research in fault detection and diagnosis (FDD) [4, 9, 10, 29, 34] over the last two decades. Such efforts have led to the development of many FDD techniques, unfortunately, little attention has been paid to the related problem, i.e., reconfigurable fault-tolerant control, until the mid-1980s [8, 17]. Only recently, the fault-tolerant control problem has begun to receive more attention [3, 14, 15, 27, 28, 35, 37].

A fault-tolerant control system (FTCS) is a control system that possesses the ability to accommodate system failures *automatically*, and to maintain overall system stability and acceptable performance. Generally speaking, fault-tolerant control systems can be classified as *passive* [15, 33] and *active* [17]. An active fault-tolerant control system compensates for faults either by selecting a precomputed control law (projection-based approaches) [19, 21] or by synthesizing a new control strategy on-line (on-line automatic controller redesign approaches) [17]. Both approaches use FDD schemes to detect and diagnose faults and to activate control reconfiguration mechanisms. Such systems are also known as reconfigurable [11, 13, 19], restructurable [12, 17], or self-repairing control systems [8]. Typically, an active FTCS consists of three parts: a reconfigurable controller, an FDD scheme, and a control law reconfiguration mechanism. Key issues are how to design: 1) a robust reconfigurable controller, 2) an FDD scheme with high sensitivity to faults and robustness to model uncertainties and external disturbances, and 3) a reconfiguration mechanism which can organize the reconfigured controller in such a way that the prefault system performance can be recovered to the maximum extent. This work focuses on the development of a new integrated approach to active fault-tolerant control system design.

In general, the existing active fault-tolerant control system design methods can be categorized based on the following approaches: linear quadratic regulator (LQR) [17, 21]; eigenstructure assignment (EA) [13]; multiple model (MM) [7, 19, 24, 31]; adaptive control [6, 31]; pseudo-inverse [11]; model following [12, 22]; and neural networks [23]. Among these, the study on MM-based reconfigurable control has drawn increasing attention recently [7, 19, 24, 30, 31]. One of the approaches developed in [19], known as MM adaptive estimator/MM adaptive control (MMAE/MMAC), synthesizes each of the reconfigurable controllers using LQR technique. In this approach, the system under the presumed failure modes is represented by a set of models, and a bank of Kalman filters is used to estimate the states of the system based on the presumed failure modes.

Innovation sequence of each Kalman filter is used to calculate the probabilities of individual failures, and the aggregated state estimate and the control input are the probability-weighted average of the signals from each model. However, in the above scheme, there is no interaction among Kalman filters. Such an approach is effective in dealing with problems with an unknown structure or parameter but without structural or parametric changes. Obviously, the problem of fault diagnosis and reconfigurable control does not fit well into such a framework because, in general, the system structure or parameters do change as a component or subsystem fails. To overcome this weakness and to make MM algorithms more suitable for the current problem, an interacting MM (IMM) FDD approach has been proposed recently [36]. In this approach, the occurrence or the recovery of a failure in a dynamic system has been explicitly modeled as a finite-state Markov chain with known transition probabilities. Since changes of the system are explicitly considered and effectively handled in the IMM algorithm, it has been shown that the IMM algorithm is much superior in performing FDD than other existing methods [36].

Typically, faults can occur in system components, actuators, and sensors. Due to the inherent difficulties in considering all types of failures simultaneously, existing single-model-based approaches consider these faults separately. Using the MM approach, however, the system component, actuator, and sensor faults can be dealt with simultaneously. In this paper, FDD and reconfigurable control in the presence of all three types of faults have been addressed.

The objective of this work is to extend the proposed IMM-based FDD approach to the design of an integrated FDD and reconfigurable control. In the proposed scheme, the IMM estimator is utilized to provide the information on FDD, as well as the state estimation. The reconfiguration mechanism is based on a suitable combination of the information from the mode probability in the IMM algorithm and a system performance index. Since the stability and dynamic behavior of the closed-loop system can be described by its eigenvalues and corresponding eigenvectors, i.e. eigenstructure, recovery of the dynamic performance after the faults can be achieved via assigning the eigenstructure of the reconfigured system as close to that of the prefault system as possible if the redundant control is available [15]. A set of reconfigurable control laws is synthesized using an EA technique. In addition, to achieve zero steady-state tracking even in the presence of faults, a set of feedforward control laws is also designed using an input weighting technique [13]. Fig. 1 depicts the structure of the scheme.

The paper is organized as follows. In Section II, modeling of system component, actuator, and sensor faults is presented. Based on IMM estimator, FDD mechanisms are outlined in Section III. Section IV discusses the reconfigurable controller design and

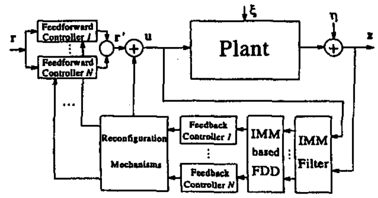

Fig. 1. General structure of proposed FDD and reconfigurable control scheme.

implementation issues. In Section V, performance evaluation of the proposed scheme for an aircraft is presented. Conclusions are drawn in Section VI.

II. REPRESENTATION OF FAILURES IN SYSTEM COMPONENTS, ACTUATORS AND SENSORS

A. Hidden Markov Chain Model for Systems with Failures

Suppose that a discrete-time process which represents the possible system structural/parametric changes due to failures is represented by a first-order Markov chain with state $m(k)$ taking values in a finite set $\mathcal{S} = 1,2,\ldots,s$. At each time step, the transition probabilities of the chain can be defined by

$$\pi_{ij}(k) = P\{m(k) = j \mid m(k-1) = i\} \qquad \forall \quad i,j \in \mathcal{S} \tag{1}$$

with

$$\sum_{j\in\mathcal{S}} \pi_{ij}(k) = 1, \qquad i = 1,\ldots,s \tag{2}$$

where $P\{\cdot\}$ denotes the probability; $m(k)$ is the discrete-valued *modal state* (i.e., the indicator of the normal or the fault mode) at time k; π_{ij} is the transition probability from the mode i to the mode j; the event that m_j is in effect at time k is denoted as $m_j(k) \triangleq \{m(k) = j\}$.

The model of the system with potential failures can be expressed as

$$\mathbf{x}(k+1) = F(k,m(k+1))\mathbf{x}(k) + G(k,m(k+1))\mathbf{u}(k) + \Gamma(k,m(k+1))\xi(k,m(k+1)) \tag{3}$$

$$\mathbf{z}(k) = H(k,m(k))\mathbf{x}(k) + \eta(k,m(k)) \tag{4}$$

where $\mathbf{x} \in \mathcal{R}^n$ is the state vector; $\mathbf{z} \in \mathcal{R}^p$ is the measurement vector; $\mathbf{u} \in \mathcal{R}^l$ is the control input vector; $\xi(k) \in \mathcal{R}^n$ and $\eta(k) \in \mathcal{R}^p$ are independent discrete-time random process with mean $\bar{\xi}(k)$ and $\bar{\eta}(k)$ and covariances $Q(k)$ and $R(k)$, representing system and measurement noises, respectively. It is assumed that the initial state has a mean $\bar{\mathbf{x}}_0$ and a covariance $\bar{P}_0$, and they are independent from $\xi(k)$ and $\eta(k)$.

The system (3)–(4) is known as a "jump linear system" [16, 36]. It can be seen from (4) that the state observations are noisy and mode dependent.

Therefore, the mode information is imbedded in the measurement sequence. In other words, the system mode sequence is an indirectly observed (or hidden) Markov chain.

B. Multiple-Model Representation of System Failures

Based on the system model (3)–(4), it is possible to represent different failures in the system. Even though the MM method is a suitable choice for FDD and reconfigurable control, the way to choose a good model set to represent all possible fault situations (including fault types, number of faults, and fault magnitude) is crucial for the success in FDD and reconfigurable control design. Generally speaking, the performance of an MM algorithm depends on the model set used.

Assume that a set of N models has been used to represent the normal and $N-1$ different failure situations, then the system in (3)–(4) can further be represented as

$$\begin{aligned}\mathbf{x}(k+1) &= (F(k)+\Delta F_j(k))\mathbf{x}(k)\\ &\quad + (G(k)+\Delta G_j(k))\mathbf{u}(k) + \Gamma_j(k)\boldsymbol{\xi}_j(k)\\ &= F_j(k)\mathbf{x}(k) + G_j(k)\mathbf{u}(k) + \Gamma_j(k)\boldsymbol{\xi}_j(k) \qquad (5)\end{aligned}$$

$$\begin{aligned}\mathbf{z}(k) &= (H(k)+\Delta H_j(k))\mathbf{x}(k) + \boldsymbol{\eta}_j(k)\\ &= H_j(k)\mathbf{x}(k) + \boldsymbol{\eta}_j(k) \qquad j = 1,\ldots,N \qquad (6)\end{aligned}$$

where $\Delta F_j(k), \Delta G_j(k)$ and $\Delta H_j(k)$ ($j = 2,\ldots,N$) represent the fault-induced changes in the system components, actuators, and sensors, respectively. They should be null matrices when $j = 1$. The subscript j denote quantities pertaining to the model $m_j \in \mathcal{M}$. $\mathcal{M} = [m_1, m_2, \ldots, m_N]$ is a set of all system models representing the normal system and the system with all considered faults. Matrices $F_j(k)$, $G_j(k)$, and $H_j(k)$ correspond to the jth postfault models of the system.

The objective of the integrated FDD and reconfigurable controller is to estimate the state and to identify the system mode in effect from a sequence of noise-corrupted observations, and then to recover the performance of the prefault system by selecting an appropriate controller among a set of precomputed controllers.

III. FAULT DETECTION, DIAGNOSIS AND CONTROLLER RECONFIGURATION MECHANISMS

A. State Estimation and Fault Diagnosis Using IMM Estimator

The IMM estimator [5] is generally considered to be one of the most cost-effective schemes for state estimation involving both continuous and discrete states [16]. It has been successfully used in a number of applications, e.g. maneuvering target tracking [16, 20], and FDD [36].

The IMM algorithm is a recursive estimator with the following steps in each iteration:

1) interaction of the model-conditional estimates,
2) model-conditional filtering,
3) mode probability update,
4) estimates combination.

In the first step, the input to the filter matched to a certain mode is obtained by mixing the estimates of all filters from the previous iteration under the assumption that this particular mode is in effect at the present time; a bank of filters corresponding to different models is calculated in parallel in the second step; mode probability is then updated based on the model-conditional innovations and the likelihood functions; finally, the aggregated state estimate is obtained as a probability-weighted sum of the updated state estimates from all the filters.

The probability of the mode in effect plays a key role in determining the weights in the combination of state estimates and covariances for aggregated state estimate. It should be pointed out that in comparison with the existing noninteracting MM algorithms, the step 1 is unique for the IMM estimator. It is because of this mixture of the estimates that makes the estimation for the state and identification for the system mode more responsive to the system changes, thus leads to significantly better FDD performance [36].

Fig. 2 shows a block diagram of the IMM estimator for FDD. From this diagram, inherent relations of the above four steps can be observed clearly.

B. Fault Detection and Diagnosis Scheme

In active FTCS, timely and correct detection and diagnosis of a fault is crucial for good performance. Using the IMM estimator, it is effective to use the mode probabilities to provide an indication of the mode in effect at a given time. Hence, it can be used as an index for FDD. The fault detection decision can be made by the following rule:

$$\mu_j(k+1) = \max_i \mu_i(k+1) \begin{cases} > \mu_T \Rightarrow H_j : \text{fault } j \text{ occurred} \\ \le \mu_T \Rightarrow H_1 : \text{no fault} \end{cases} \qquad (7)$$

where μ_T, $0 < \mu_T < 1$, is the detection threshold.

A complete cycle of the IMM-based FDD scheme with Kalman filters as its mode-matching filters is summarized in Table I.

C. Integrated Fault Detection, Diagnosis, and Controller Reconfiguration Mechanisms

It has been shown in [36] that, in comparison with noninteracting MM approaches, the IMM-based FDD

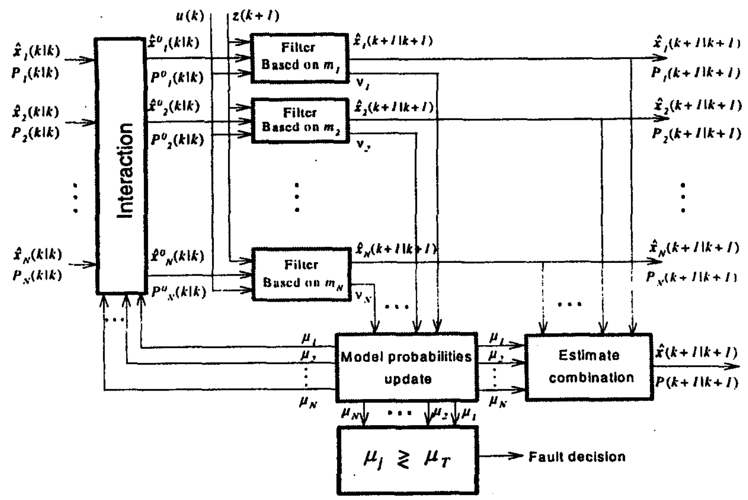

Fig. 2. Block diagram of IMM-based FDD approach.

approach provides a faster and more reliable detection and diagnosis for system failures. However, these conclusions were drawn only for open-loop systems. When a control action is introduced and combined with an MM estimator to form a closed-loop system, the effect of the feedback will force the residuals from different models to be similar and this affects the discrimination property of the filter. Such a situation is even more serious in reconfigurable control design because the objective of a reconfigurable control is to make the performance of the reconfigured system as close to that of the prefault system as possible. Such a design principle inherently leads to similar residuals in each filter and may make the FDD provided only by the mode probability less reliable.

To overcome such a drawback, various heuristic techniques have been investigated, e.g. the addition of probing signals, alternative computation of probabilities, bounded conditional probabilities, Kalman filter retuning, scalar penalty increase, probability smoothing, and increased residual propagation [2, 18, 19, 32]. These techniques may enhance the performance of FDD and lead to subsequent improvement in control to some extent. However, preliminary investigation has shown that these techniques are not effective in the current situation. This motivates us to develop a new method for more reliable FDD and reconfigurable control.

Inspired by the MMs' switching and tuning approach proposed in [25], a performance index is used to provide additional information for reliable fault diagnosis and controller reconfiguration. This index is calculated as

$$J_j(k+1) = c_1\varepsilon_j^2(k+1) + c_2 \sum_{i=k-M+2}^{k+1} \varepsilon_j^2(i) \tag{8}$$

where ε_j is the 2-norm of the filter residual vector corresponding to the jth model, defined by

$$\varepsilon_j(k+1) = \|\mathbf{z}(k+1) - H_j(k+1)\hat{\mathbf{x}}_j(k+1 \mid k+1)\|_2 \tag{9}$$

where $\mathbf{z}(k+1)$ is the measurement at time $(k+1)$, $\hat{\mathbf{x}}_j(k+1 \mid k+1)$ denotes the estimation of the state of the closed-loop system at time $(k+1)$ for the model j. $c_1 \geq 0$ and $c_2 \geq 0$ are constants. They determine the relative weights given to the instantaneous and accumulative measures. To consider the time-varying nature of the problem and to make the performance measure more responsive to fault-induced changes, a moving window of length M has been used in the second term in (8).

Based on the above analysis, for reliable fault diagnosis and control system reconfiguration, the following condition can be used to activate the reconfiguration process:

$$\begin{cases} \mu_j(k+1) = \max_i \mu_i(k+1) > \mu_T \quad \text{and} \\ j = \arg\min_i J_i(k+1) \Rightarrow \mathcal{H}_j : \text{reconfiguration for fault } j \\ \mu_j(k+1) = \max_i \mu_i(k+1) \leq \mu_T \\ \qquad \Rightarrow \mathcal{H}_1 : \text{no reconfiguration} \end{cases} \tag{10}$$

D. Structure of Integrated FDD and Reconfigurable Control

A block diagram of the combined IMM-based FDD and the reconfigurable control scheme is shown in Fig. 3. Based on the on-line FDD information, the real-time reconfiguration can be carried out.

Similar to the aggregated state estimation in the IMM estimator, the aggregated control signal, $\mathbf{u}(k)$,

TABLE I
One Cycle of IMM-Based FDD Scheme

Consider the following system (for $j = 1, 2, ..., N$):

$$x(k+1) = F_j(k)x(k) + G_j(k)u(k) + \Gamma_j(k)\xi_j(k)$$
$$z(k+1) = H_j(k+1)x(k+1) + \eta_j(k+1)$$

with $\xi_j(k)=\mathcal{N}[\bar{\xi}_j(k), Q_j(k)]$; $\eta_j(k+1)=\mathcal{N}[\bar{\eta}_j(k+1), R_j(k+1)]$; $x_j(0)=\mathcal{N}[\bar{x}_0, \bar{P}_0]$.

1. Interaction/Mixing of the estimates (for $j = 1, 2, ..., N$):

predicted mode probability: $\mu_j(k+1|k) \triangleq P\{m_j(k+1)|z^k\} = \sum_i \pi_{ij}\mu_i(k)$

mixing probability: $\mu_{i|j}(k) \triangleq P\{m_i(k)|m_j(k+1), z^k\} = \pi_{ij}\mu_i(k)/\mu_j(k+1|k)$

mixing estimate: $\hat{x}_j^0(k|k) \triangleq E[x(k)|m_j(k+1), z^k] = \sum_i \hat{x}_i(k|k)\mu_{i|j}(k)$

mixing covariance: $P_j^0(k|k) \triangleq \text{cov}[\hat{x}_j^0(k|k)|m_j(k+1), z^k]$

$$= \sum_i \left[P_i(k|k) + [\hat{x}_j^0(k|k) - \hat{x}_i(k|k)][\hat{x}_j^0(k|k) - \hat{x}_i(k|k)]^T\right] \mu_{i|j}(k)$$

2. Model-conditional filtering (for $j = 1, 2, ..., N$):

predicted state (from k to $k+1$):

$$\hat{x}_j(k+1|k) \triangleq E[x(k+1)|m_j(k+1), z^k] = F_j(k)\hat{x}_j^0(k|k) + G_j(k)u(k) + \Gamma_j(k)\bar{\xi}_j(k)$$

predicted covariance:

$$P_j(k+1|k) \triangleq \text{cov}[\hat{x}_j(k+1|k)|m_j(k+1), z^k] = F_j(k)P_j^0(k|k)F_j(k)^T + \Gamma_j(k)Q_j(k)\Gamma_j(k)^T$$

measurement residual: $\nu_j \triangleq z(k+1) - E[z(k+1)|m_j(k+1), z^k]$

$$= z(k+1) - H_j(k+1)\hat{x}_j(k+1|k) - \bar{\eta}_j(k+1)$$

residual covariance: $S_j \triangleq E[\nu_j|m_j(k+1), z^k] = H_j(k+1)P_j(k+1|k)H_j(k+1)^T + R_j(k+1)$

filter gain: $K_j = P_j(k+1|k)H_j(k+1)^T S_j(k+1)^{-1}$

updated state: $\hat{x}_j(k+1|k+1) \triangleq E[x(k+1)|m_j(k+1), z^{k+1}] = \hat{x}_j(k+1|k) + K_j\nu_j$

updated covariance:

$$P_j(k+1|k+1) \triangleq \text{cov}[\hat{x}_j(k+1|k+1)|m_j(k+1), z^{k+1}] = P_j(k+1|k) - K_j(k+1)S_j(k+1)K_j(k+1)^T$$

3. Mode probability update and FDD logic (for $j = 1, 2, ..., N$):

likelihood function: $L_j(k+1)=\mathcal{N}[\nu_j(k+1); 0, S_j(k+1)]$

$$= \frac{1}{\sqrt{|(2\pi)S_j(k+1)|}}\exp\left[-\tfrac{1}{2}\nu_j(k+1)^T S_j^{-1}(k+1)\nu_j(k+1)\right]$$

mode probability: $\mu_j(k+1) \triangleq P\{m_j(k+1)|z^{k+1}\} = \frac{\mu_j(k+1|k)L_j(k+1)}{\sum_i \mu_i(k+1|k)L_i(k+1)}$

FDD decision: $\mu_j(k+1) = \max_i \mu_i(k+1) \begin{cases} > \mu_T \Rightarrow H_j : \text{fault } j \text{ occurred} \\ \leq \mu_T \Rightarrow H_1 : \text{no fault} \end{cases}$

4. Combination of estimates:

aggregated estimate: $\hat{x}(k+1|k+1) \triangleq E[x(k+1)|z^{k+1}] = \sum_j \hat{x}_j(k+1|k+1)\mu_j(k+1)$

aggregated covariance:

$$P(k+1|k+1) \triangleq E\left[[x(k+1) - \hat{x}(k+1|k+1)][x(k+1) - \hat{x}(k+1|k+1)]^T|z^{k+1}\right]$$
$$= \sum_j \left[P_j(k+1|k+1) + [\hat{x}(k+1|k+1) - \hat{x}_j(k+1|k+1)][\hat{x}(k+1|k+1) - \hat{x}_j(k+1|k+1)]^T\right] \mu_j(k+1)$$

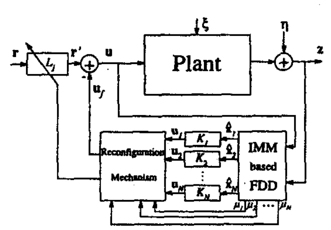

Fig. 3. Block diagram of IMM-based FDD and reconfigurable control.

can also be calculated as the probability-weighted average of each controller output, which is given by

$$\mathbf{u}(k) = \mathbf{r}'(k) - \mathbf{u}_f(k)$$
$$= \sum_{i=1}^{N}\{L_i\mathbf{r}(k) - \mathbf{u}_i(k)\} \cdot \mu_i(k) \qquad (11)$$

where $\mathbf{u}_i(k) = K_i\hat{\mathbf{x}}_i(k \mid k)$ is the feedback control law designed for the ith model in the model set, $\hat{\mathbf{x}}_i(k \mid k)$ is the corresponding state estimate obtained by the ith Kalman filter. K_i and L_i are the feedback and the feedforward control gains corresponding to the ith model. $\mu_i(k)$ denotes the corresponding mode probability for the ith model.

IV. RECONFIGURABLE CONTROLLER DESIGN AND ON-LINE CONTROLLER RECONFIGURATION

A. Dynamic Performance Recovery-Feedback Controller Design

LQR and EA are among the most popular controller design techniques for multiinput and multioutput systems. The advantage of EA is that when the performance specifications are given in terms of system eigenstructure, the eigenstructure can be achieved exactly for the stability and desired dynamic performance. The condition for the exact assignment is that there is a sufficient number of actuators and measurements available and that the desired eigenvectors reside in the achievable subspace [1]. The limitation of EA is that the system performance is not optimal in any measure. The LQR could be used to optimize the controller design by minimizing a quadratic function of the system response and the control energy. In general, the LQR-based control design will guarantee the closed-loop system stability and certain degree of robustness, but may not easily achieve the specific system performance due to ambiguities in the selection of the weighting matrices. For the above reasons, the EA is used for the design of the reconfigurable controller while LQR is used for the design of the nominal controller.

1) *Assignment for the Best Eigenvalues and Eigenvectors*: Suppose that the dynamics of the system have undergone some changes due to faults in system components, actuators, and sensors, and the system models with normal and different faulty conditions have become

$$\mathbf{x}(k+1) = F_j\mathbf{x}(k) + G_j\mathbf{u}(k), \qquad j = 1,\ldots,N. \quad (12)$$

The aim of reconfigurable control system design is to synthesize a set of new feedback gain matrices so that the closed-loop eigenvalues of the reconfigured system are the same as those of the prefault system, i.e.,

$$\lambda_j^i = \lambda(F_j + G_jK_j) = \lambda^i = \lambda(F_1 + G_1K_1), \quad i = 1,\ldots,n, \quad j = 2,\ldots,N. \quad (13)$$

where K_1 denotes a control gain matrix designed for the nominal (fault-free) system, and K_j, $j = 2,\ldots,N$, represents the new feedback control gain matrices under different fault conditions. $\lambda(\cdot)$ denotes the eigenvalues of the system.

The closed-loop system eigenvectors of the reconfigured system, $\{\mathbf{v}_j^i,\ i = 1,\ldots,n,\ j = 2,\ldots,N\}$, with the feedback gain matrix K_j will satisfy

$$(F_j + G_jK_j)\mathbf{v}_j^i = \lambda_j^i\mathbf{v}_j^i \quad (14)$$

or

$$\mathbf{v}_j^i = (\lambda_j^iI - F_j)^{-1}G_jK_j\mathbf{v}_j^i. \quad (15)$$

Then, the objective of the reconfigurable control system is to synthesize a feedback gain matrix K_j such that the eigenvectors of reconfigured closed-loop system $\mathbf{v}_j^i$ is as close to the corresponding eigenvectors of the prefault system $\mathbf{v}_1^i$ as possible. Because of the variations in system dynamics, in general, $\mathbf{v}_j^i$ does not lie in the same subspace as $\mathbf{v}_1^i$, which may be viewed as the desired eigenvector for $\mathbf{v}_j^i$. The best possible closed-loop system eigenvector can be obtained by the projection of the desired eigenvector onto the subspace spanned by the columns of $(\lambda_j^iI - F_j)^{-1}G_j$. In the context of reconfigurable control system design, the best choice of $\mathbf{v}_j^i$ can be obtained by projecting the corresponding $\mathbf{v}_1^i$ onto E_j^i orthogonally, where E_j^i and a new vector $\mathbf{w}_j^i$ can be defined as

$$E_j^i = (\lambda_j^iI - F_j)^{-1}G_j \quad (16)$$

$$\mathbf{w}_j^i = K_j\mathbf{v}_j^i. \quad (17)$$

Consequently, (15) can be rewritten as

$$\mathbf{v}_j^i = E_j^i\mathbf{w}_j^i. \quad (18)$$

The desired eigenvector $\mathbf{v}_j^i$ in the achievable subspace can be found by the following least-squares minimization

$$\begin{aligned}\min J_i(\mathbf{v}_j^i) &= \min\{(\mathbf{v}_j^i - \mathbf{v}_1^i)^T W_j^i(\mathbf{v}_j^i - \mathbf{v}_1^i)\}\\ &= \min\{(E_j^i\mathbf{w}_j^i - \mathbf{v}_1^i)^T W_j^i(E_j^i\mathbf{w}_j^i - \mathbf{v}_1^i)\},\\ &\qquad i = 1,\ldots,n, \quad j = 2,\ldots,N \quad (19)\end{aligned}$$

and

$$\mathbf{v}_j^i = E_j^i(E_j^{iT}W_j^{iT}W_j^iE_j^i)^{-1}E_j^{iT}W_j^{iT}\mathbf{v}_1^i \quad (20)$$

where $W_j^i \in \mathcal{R}^{n\times n}$ is a positive definite weighting matrix. Suggestions about how to choose weighting matrix W_j^i are given in [13].

2) *Computation of the Reconfigurable Control Gain Matrix*: Consider the following closed-loop reconfigured system equation

$$\mathbf{x}_{k+1} = (F_j + G_jK_j)\mathbf{x}_k. \quad (21)$$

To simplify the procedure in calculating the matrix K_j, a linear transformation matrix

$$\Omega_j = [G_j \ \vdots\ \Theta_j] \in \mathcal{R}^{n\times n} \quad (22)$$

is chosen, where $\Theta_j \in \mathcal{R}^{n\times(n-l)}$ is an arbitrary matrix such that $\mathrm{rank}(\Omega_j) = n$.

Applying the linear transformation Ω_j to (21), a new set of state variables $\bar{\mathbf{x}}_k \in \mathcal{R}^n$ can be obtained

$$\bar{\mathbf{x}}_k = \Omega_j^{-1}\mathbf{x}_k. \quad (23)$$

Thus (21) is transformed to

$$\bar{\mathbf{x}}_{k+1} = (\bar{F}_j + \bar{G}_jK_j\Omega_j)\bar{\mathbf{x}}_k \quad (24)$$

where

$$\bar{F}_j = \Omega_j^{-1}F_j\Omega_j, \qquad \bar{G}_j = \Omega_j^{-1}G_j = \begin{bmatrix} I_l \\ 0 \end{bmatrix}.$$

The corresponding eigenvectors under this transformation are related by

$$\bar{\mathbf{v}}_j^i = \Omega_j^{-1}\mathbf{v}_j^i = \begin{bmatrix} \mathbf{s}^i \\ \mathbf{g}^i \end{bmatrix}.$$

Clearly, the eigenvalues, eigenvectors and system matrices satisfy

$$(\overline{F}_j + \overline{G}_j K_j \Omega_j)\overline{\mathbf{v}}_j^i = \lambda_j^i \overline{\mathbf{v}}_j^i, \qquad i = 1,\ldots,n, \quad j = 2,\ldots,N. \tag{25}$$

Equation (25) can be rearranged as follows

$$(\lambda_j^i I - \overline{F}_j)\overline{\mathbf{v}}_j^i = \overline{G}_j K_j \Omega_j \overline{\mathbf{v}}_j^i, \qquad i = 1,\ldots,n, \quad j = 2,\ldots,N. \tag{26}$$

By exploiting the special structure of $\overline{G}_j$, we can rewrite (26) as

$$\left[\begin{array}{c|c} \lambda_j^i I_l - \overline{F}_{11} & -\overline{F}_{12} \\ \hline -\overline{F}_{21} & \lambda_j^i I_{n-l} - \overline{F}_{22} \end{array}\right] \left[\begin{array}{c} \mathbf{s}^i \\ \hline \mathbf{g}^i \end{array}\right] = \left[\begin{array}{c} I_l \\ \hline 0 \end{array}\right] K_j \Omega_j \left[\begin{array}{c} \mathbf{s}^i \\ \hline \mathbf{g}^i \end{array}\right] \tag{27}$$

where

$$\overline{F}_j = \left[\begin{array}{c|c} \overline{F}_{11} & \overline{F}_{12} \\ \hline \overline{F}_{21} & \overline{F}_{22} \end{array}\right] = \Omega_j^{-1} F_j \Omega_j.$$

The first matrix equation in the partitioned form in (27) can be written as

$$(\lambda_j^i I_l - \overline{F}_{11})\mathbf{s}^i - \overline{F}_{22}\mathbf{g}^i = K_j \Omega_j \left[\begin{array}{c} \mathbf{s}^i \\ \hline \mathbf{g}^i \end{array}\right]$$

$$i = 1,\ldots,n, \quad j = 2,\ldots,N. \tag{28}$$

Further, by letting $\overline{F}_1 = [\overline{F}_{11} \quad \overline{F}_{12}]$, (28) becomes

$$[\overline{F}_1 + K_j \Omega_j]\overline{\mathbf{v}}_j^i = \lambda_j^i \mathbf{s}^i, \qquad i = 1,\ldots,n, \quad j = 2,\ldots,N \tag{29}$$

or, in a compact form

$$[\overline{F}_1 + K_j \Omega_j]\overline{V}_j = S_j \tag{30}$$

where $\overline{V}_j = [\overline{\mathbf{v}}_j^1 \; \overline{\mathbf{v}}_j^2 \; \ldots \; \overline{\mathbf{v}}_j^n] \in \mathcal{R}^{n\times n}$, and $S_j = [\lambda_j^1 \mathbf{s}^1 \; \lambda_j^2 \mathbf{s}^2 \; \ldots \; \lambda_j^n \mathbf{s}^n] \in \mathcal{R}^{l\times n}$.

It should be noted that $\overline{V}_j$ and S_j are often complex. To alleviate the need for complex arithmetic, a transformation is needed to transform $\overline{V}_j$ and S_j to real matrices. Assume that $\lambda_j^i = (\lambda_j^{i+1})^*$ and $\overline{\mathbf{v}}_j^i = (\overline{\mathbf{v}}_j^{i+1})^*$, and assuming all remaining eigenvalues are real, we can define a transformation matrix

$$\Phi_j = \left[\begin{array}{c|cc|c} I & 0 & 0 & 0 \\ \hline 0 & 1/2 & -j1/2 & 0 \\ 0 & 1/2 & j1/2 & 0 \\ \hline 0 & 0 & 0 & I \end{array}\right] \in \mathcal{R}^{n\times n}. \tag{31}$$

Multiplying both sides of (30) by the transformation matrix Φ_j, i.e.,

$$[\overline{F}_1 + K_j \Omega_j]\overline{V}_j \Phi_j = S_j \Phi_j \tag{32}$$

will transform $\overline{V}_j$ and S_j to real matrices and at the same time not alter the calculation of the feedback gain matrix. Note that for the case of more than one pair of self-conjugate eigenvalues, the corresponding rows and columns in the Φ_j matrix need to be assigned by the transformation matrix

$$\Phi_0 = \begin{bmatrix} 1/2 & -j1/2 \\ 1/2 & j1/2 \end{bmatrix}$$

in place of unity matrix I.

From (30) the desired feedback gain matrix can be calculated as

$$K_j = (S_j - \overline{F}_1 \overline{V}_j)(\Omega_j \overline{V}_j)^{-1}, \qquad j = 2,\ldots,N \tag{33}$$

or from (32), the desired feedback gain matrix for the case of complex eigenvalues can be obtained as

$$K_j = (S_j \Phi_j - \overline{F}_1 \overline{V}_j \Phi_j)(\Omega_j \overline{V}_j \Phi_j)^{-1}, \qquad j = 2,\ldots,N. \tag{34}$$

B. Steady-State Performance Recovery-Feedforward Controller Design

Even though the dynamic performance of the prefault system can be recovered to the maximum extent with EA, it is also important to consider the steady-state performance. This can be accomplished by a set of properly designed feedforward control gains L_j, $j = 1,\ldots,N$ [13]. These gains can be calculated as follows using a property of z-transform.

Suppose that the original reference input $\mathbf{r}(k)$ has been scaled by a set of input weighting matrices L_j, as $\mathbf{r}'(k)$ for the jth model in the model set, then we have

$$\mathbf{r}_j'(k) = L_j \cdot \mathbf{r}(k), \qquad j = 1,\ldots,N. \tag{35}$$

The steady-state output of the stable closed-loop system subject to a unit step input can be calculated using the final value theorem in z-transform:

$$\begin{aligned} \mathbf{y}(\infty) &= \lim_{k\to\infty} \mathbf{y}(k) = \lim_{k\to\infty} H_c \mathbf{x}(k) \\ &= \lim_{z\to 1}(z-1)\Phi_j(z) L_j R(z) \\ &= \left\{\lim_{z\to 1} H_c (zI - F_j + G_j K_j)^{-1} G_j\right\} L_j \\ &= \Psi_j L_j \qquad j = 1,\ldots,N \end{aligned} \tag{36}$$

where K_j, $j = 1,\ldots,N$, represent the jth feedback control gains. H_c is a matrix such that the system output $\mathbf{y}(k) = H_c \mathbf{x}(k)$ tracks the reference input $\mathbf{r}(k)$. $\Psi_j = \{\lim_{z\to 1} H_c (zI - F_j + G_j K_j)^{-1} G_j\}$ is the steady-state gain of the system before scaling.

The steady-state performance recovery problem can then be stated as choosing appropriate matrices $L_j \in \mathcal{R}^{l\times l}$ to minimize $J(L_j)$

$$\min_{L_j} J(L_j) = \min_{L_j} \|I - \Psi_j L_j\|, \qquad j = 1,\ldots,N. \tag{37}$$

If Ψ_j is invertible, then

$$L_j = \left\{ \lim_{z\to 1} H_c(zI - F_j + G_j K_j)^{-1} G_j \right\}^{-1}, \qquad j = 1,\ldots,N. \tag{38}$$

It is important to point out that the feedforward control gains L_j are dependent upon the feedback control gain matrices K_j. It should be noted that if the number of system output is less than or equal to the number of system input, i.e., $m \le l$, the steady-state performance of the original system can be recovered completely. If $m > l$, the chosen L_j is to minimize $J(L_j)$ in a Frobenius-norm sense [13].

C. Reconfigurable Control Signal Generation Strategies

Even though in the above IMM scheme, there are a set of models and the corresponding feedback and feedforward gains for each failure mode, there is still a single control signal at any given time. In general, there are two ways to generate this signal: one is based on a Bayesian scheme and the other is by the maximum *a posteriori* (MAP) approach [19, 32].

In the former, the control signal is obtained as a probability-weighted average of the signals generated from all the models. The advantage of this approach is that it is able to reduce the effect of incorrect model selection during the early stage of reconfiguration. However, once the failure mode has been identified correctly, there is no need to continuously use the probability-weighted approach, as the non-zero probabilities (due to noise) can have adverse effects on the control signal generation.

In the MAP approach, the control signal is selected from the model which has the highest probability. The risk of this approach is that during the transient of reconfiguration process, the model with the highest probability may not necessarily correspond to the correct failure mode. Incorrectly selected control signals can introduce further transients into the system.

Clearly, a combination of these two approaches would be advantageous. To be more specific, during the transient period, the Bayesian approach is used. Once the failure has been detected and diagnosed with some degree of certainty, the control signal from the model with the highest probability will be used. In summary, this combined decision rule can be described as follows:

if $\mu_j(k) \le \mu_T$

$$\mathbf{u}(k) = \sum_{i=1}^{N} \{L_i \mathbf{r}(k) - \mathbf{u}_i(k)\} \cdot \mu_i(k) \tag{39}$$

otherwise

$$\mathbf{u}(k) = L_j \mathbf{r}(k) - \mathbf{u}_j(k), \qquad j = \arg\max_i \mu_i(k)$$

where μ_T denotes the threshold which takes the same value as in (10).

V. PERFORMANCE EVALUATION OF THE PROPOSED SCHEME FOR AN AIRCRAFT

The effectiveness of the proposed scheme is demonstrated in this section through a longitudinal vertical takeoff and landing (VTOL) aircraft model [26].

A. Aircraft Model

The linearized model of the aircraft can be described by

$$\begin{aligned} \dot{\mathbf{x}}(t) &= A\mathbf{x}(t) + B\mathbf{u}(t) + \boldsymbol{\xi}(t) \\ \mathbf{z}(t) &= C\mathbf{x}(t) + \boldsymbol{\eta}(t) \end{aligned} \tag{40}$$

where $\mathbf{x} = [V_h\ V_v\ q\ \theta]^T$, $\mathbf{u} = [\delta_c\ \delta_l]^T$. The states and the inputs are: horizontal velocity V_h, vertical velocity V_v, pitch rate q, and pitch angle θ; collective pitch control δ_c, and longitudinal cyclic pitch control δ_l. The model parameters are given as follows

$$A = \begin{bmatrix} -0.0366 & 0.0271 & 0.0188 & -0.4555 \\ 0.0482 & -1.01 & 0.0024 & -4.0208 \\ 0.1002 & 0.3681 & -0.707 & 1.420 \\ 0.0 & 0.0 & 1.0 & 0.0 \end{bmatrix},$$

$$B = \begin{bmatrix} 0.4422 & 0.1761 \\ 3.5446 & -7.5922 \\ -5.52 & 4.49 \\ 0.0 & 0.0 \end{bmatrix}, \qquad C = \begin{bmatrix} 1 & 0 & 0 & 0 \\ 0 & 1 & 0 & 0 \\ 0 & 0 & 1 & 0 \\ 0 & 1 & 1 & 1 \end{bmatrix}.$$

The zero hold equivalent system can be represented by

$$\begin{aligned} \mathbf{x}(k+1) &= F\mathbf{x}(k) + G\mathbf{u}(k) + \boldsymbol{\xi}(k) \\ \mathbf{z}(k) &= H\mathbf{x}(k) + \boldsymbol{\eta}(k) \end{aligned} \tag{41}$$

where $F = e^{AT}$, $G = (\int_0^T e^{A\tau} d\tau)B$, $H = C$, and the sampling period $T = 0.1$ s.

Parameters are given as follows. $Q = \mathrm{diag}\{0.01^2, 0.01^2, 0.01^2, 0.01^2\}$, $R = \mathrm{diag}\{0.2^2, 0.2^2\}$, $\mathbf{x}_0 = [250\ 50\ 10\ 8]^T$. The external control input is selected as $\mathbf{u} = [100\ 100]^T$. Initial parameters for the Kalman filters in the filter bank are $\hat{\mathbf{x}}_j^0 = \mathbf{x}_0$, $P_j^0 = 99I$, $Q_j = Q$, and $R_j = 2R, \forall j = 1,\ldots,N$. The nominal controller is designed using LQR, the state and control weighting matrices are chosen as $Q_{\mathrm{LQR}} = \mathrm{diag}\{1,1,1,1\}$ and $R_{\mathrm{LQR}} = \mathrm{diag}\{1,1\}$.

Since the controlled variables are horizontal velocity and vertical velocity, the command tracking matrix H_c in (36) is chosen as

$$H_c = \begin{bmatrix} 1 & 0 & 0 & 0 \\ 0 & 1 & 0 & 0 \end{bmatrix}.$$

B. Fault Modeling and Model Set Design

In the following, we consider a simple situation where there is only a single failure among system

TABLE II
System Matrices for Normal and Fault Modes

Modes	F_j	G_j	H_j
Fault-free ($j=1$)	$\begin{bmatrix} 0.9964 & 0.0026 & -0.0004 & -0.0460 \\ 0.0045 & 0.9037 & -0.0188 & -0.3834 \\ 0.0098 & 0.0339 & 0.9383 & 0.1302 \\ 0.0005 & 0.0017 & 0.0968 & 1.0067 \end{bmatrix}$	$\begin{bmatrix} 0.0445 & 0.0167 \\ 0.3407 & -0.7249 \\ -0.5278 & 0.4214 \\ -0.0268 & 0.0215 \end{bmatrix}$	$\begin{bmatrix} 1.0 & 0 & 0 & 0 \\ 0 & 1.0 & 0 & 0 \\ 0 & 0 & 1.0 & 0 \\ 0 & 1.0 & 1.0 & 1.0 \end{bmatrix}$
Actuator fault ($j=2$)	$\begin{bmatrix} 0.9964 & 0.0026 & -0.0004 & -0.0460 \\ 0.0045 & 0.9037 & -0.0188 & -0.3834 \\ 0.0098 & 0.0339 & 0.9383 & 0.1302 \\ 0.0005 & 0.0017 & 0.0968 & 1.0067 \end{bmatrix}$	$\begin{bmatrix} \underline{0.0045} & 0.0167 \\ \underline{0.0} & \underline{-0.3624} \\ \underline{-0.1319} & \underline{0.1053} \\ -0.0268 & 0.0215 \end{bmatrix}$	$\begin{bmatrix} 1.0 & 0 & 0 & 0 \\ 0 & 1.0 & 0 & 0 \\ 0 & 0 & 1.0 & 0 \\ 0 & 1.0 & 1.0 & 1.0 \end{bmatrix}$
System fault ($j=3$)	$\begin{bmatrix} 0.9964 & 0.0026 & -0.0004 & -0.0460 \\ 0.0045 & \underline{0.0} & -0.0188 & -0.3834 \\ 0.0098 & 0.0339 & 0.9383 & 0.1302 \\ 0.0005 & 0.0017 & 0.0968 & 1.0067 \end{bmatrix}$	$\begin{bmatrix} 0.0445 & 0.0167 \\ 0.3407 & -0.7249 \\ -0.5278 & 0.4214 \\ -0.0268 & 0.0215 \end{bmatrix}$	$\begin{bmatrix} 1.0 & 0 & 0 & 0 \\ 0 & 1.0 & 0 & 0 \\ 0 & 0 & 1.0 & 0 \\ 0 & 1.0 & 1.0 & 1.0 \end{bmatrix}$
Sensor fault ($j=4$)	$\begin{bmatrix} 0.9964 & 0.0026 & -0.0004 & -0.0460 \\ 0.0045 & 0.9037 & -0.0188 & -0.3834 \\ 0.0098 & 0.0339 & 0.9383 & 0.1302 \\ 0.0005 & 0.0017 & 0.0968 & 1.0067 \end{bmatrix}$	$\begin{bmatrix} 0.0445 & 0.0167 \\ 0.3407 & -0.7249 \\ -0.5278 & 0.4214 \\ -0.0268 & 0.0215 \end{bmatrix}$	$\begin{bmatrix} \underline{0.0} & 0 & 0 & 0 \\ 0 & 1.0 & 0 & 0 \\ 0 & 0 & 1.0 & 0 \\ 0 & 1.0 & 1.0 & 1.0 \end{bmatrix}$

component, actuator, or sensor in any given test run. Faults are simulated at $t = 5$ s in each scenario. There are 4 possible modes in total. Table II represents the system, control, and measurement matrices for each mode, with the parameter changes highlighted.

The following model transition probability matrix is used

$$\Pi = \begin{bmatrix} 87/90 & 1/90 & 1/90 & 1/90 \\ 0.1 & 0.9 & 0 & 0 \\ 0.1 & 0 & 0.9 & 0 \\ 0.1 & 0 & 0 & 0.9 \end{bmatrix}.$$

C. Indices for Performance Evaluation

In order to evaluate the performance, the following measure is used

$$e(k) = \|H_c(\mathbf{x}^{\text{normal}}(k) - \mathbf{x}^{\text{reconfigured}}(k))\|_2 \tag{42}$$

where $\mathbf{x}^{\text{normal}}(k)$ denotes the nominal closed-loop system state when there were no failures, while $\mathbf{x}^{\text{reconfigured}}(k)$ denotes the reconfigured closed-loop system state at time k.

In addition, the mean and the maximum value of $e(k)$, $\forall k \in \{1, k_{\max}\}$ are also used as overall performance indicators, i.e.,

$$\bar{e} = \frac{1}{k_{\max}} \sum_{k=1}^{k_{\max}} e(k) \tag{43}$$

$$e_{\max} = \max\{e(k)\}. \tag{44}$$

In addition to the conventional performance indices, such as false alarm (FA) and missed detection (MD), the following performance measures have also been used in this work: average percentages of correct detection and identification (CDI), incorrect fault identification (IFI), no mode detection (NMD), and detection and correct identification delay (DCID).

1) One CDI is counted if the model that is closest to the system mode (normal or fault mode) in effect at a given time has a probability higher than the threshold $\mu_T = 0.9$.

2) One IFI is counted if the model with a probability over μ_T is not the one closest to the fault mode in effect at the given time.

3) One FA is counted if the model with a probability over μ_T is not the normal mode while the normal mode is in effect at the given time.

4) One MD is counted if the normal model has the highest probability which exceeds μ_T while the system has a fault.

5) One NMD is counted if no model has a probability above μ_T.

6) DCID is the time delay that FDD takes to correctly detected and diagnosed fault.

Obviously, it is desirable to have higher CDI and lower FA, IFI, MD, and NMD. The more detailed discussions on the performance evaluation and indices for FDD can be found in [36].

Similarly, to evaluate the reconfiguration mechanism, percentages of correct reconfiguration (CR), incorrect reconfiguration (IR), and the reconfiguration delay (RD) are also used in this work.

D. Results

1) *Eigenstructures and Controller Gains*: The eigenvalues and eigenvectors of the closed-loop system in fault-free mode and different fault modes are presented in Tables III and IV, respectively. The designed controller gains are shown in Table V. It is clear that the eigenvalues under different faults are assigned exactly to those of the fault-free system, and the corresponding eigenvectors are assigned as close to those of the fault-free system as possible. To evaluate quantitatively how close the assigned

TABLE III
Eigenvalues of Designed Reconfigurable Control System

	Fault-free	System fault	Actuator fault	Sensor fault
Eigenvalues	$\begin{bmatrix} 0.3486 \\ 0.8617 + j0.0296 \\ 0.8617 - j0.0296 \\ 0.9308 \end{bmatrix}$	$\begin{bmatrix} 0.3486 \\ 0.8617 + j0.0296 \\ 0.8617 - j0.0296 \\ 0.9308 \end{bmatrix}$	$\begin{bmatrix} 0.3486 \\ 0.8617 + j0.0296 \\ 0.8617 - j0.0296 \\ 0.9308 \end{bmatrix}$	$\begin{bmatrix} 0.3486 \\ 0.8617 + j0.0296 \\ 0.8617 - j0.0296 \\ 0.9308 \end{bmatrix}$

TABLE IV
Eigenvectors of Designed Reconfigurable Control System

Modes	Eigenvectors	Misalignment in distance∠angle(rad)
Fault-free	$\begin{bmatrix} -0.0117 & -0.0902 - j0.3021 & -0.0902 + j0.3021 & -0.6365 \\ -0.7662 & 0.2193 + j0.1863 & 0.2193 - j0.1863 & 0.0597 \\ 0.6392 & 0.3966 + j0.6433 & 0.3966 - j0.6433 & 0.4486 \\ -0.0655 & -0.1587 - j0.4706 & -0.1587 + j0.4706 & -0.6245 \end{bmatrix}$	$\begin{bmatrix} 0\angle 0 \\ 0\angle 0 \\ 0\angle 0 \\ 0\angle 0 \end{bmatrix}^T$
System fault	$\begin{bmatrix} -0.1325 & -0.0918 - j0.1710 & -0.0918 + j0.1710 & -0.6132 \\ -0.7659 & -0.0644 + j0.1887 & -0.0644 - j0.1887 & 0.0245 \\ 0.6259 & -0.0415 + j0.8018 & -0.0415 - j0.8018 & 0.4606 \\ -0.0644 & -0.0922 - j0.5191 & -0.0922 + j0.5191 & -0.6412 \end{bmatrix}$	$\begin{bmatrix} 0.1215\angle 0.1216 \\ 0.5670\angle 0.5749 \\ 0.5670\angle 0.5749 \\ 0.0470\angle 0.0470 \end{bmatrix}^T$
Actuator fault	$\begin{bmatrix} 0.0246 & -0.2281 + j0.0870 & -0.2281 - j0.0870 & -0.6430 \\ -0.7680 & 0.1327 - j0.2595 & 0.1327 + j0.2595 & 0.0657 \\ 0.6397 & 0.5169 - j0.5752 & 0.5169 + j0.5752 & 0.3460 \\ 0.0173 & -0.4430 + j0.2473 & -0.4430 - j0.2473 & -0.6801 \end{bmatrix}$	$\begin{bmatrix} 0.0904\angle 0.0905 \\ 0.4774\angle 0.4821 \\ 0.4774\angle 0.4821 \\ 0.1170\angle 0.1171 \end{bmatrix}^T$
Sensor fault	$\begin{bmatrix} -0.0117 & -0.1004 - j0.2989 & -0.1004 + j0.2989 & -0.6365 \\ -0.7662 & 0.2255 + j0.1787 & 0.2255 - j0.1787 & 0.0597 \\ 0.6392 & 0.4183 + j0.6294 & 0.4183 - j0.6294 & 0.4486 \\ -0.0655 & -0.1746 - j0.4649 & -0.1746 + j0.4649 & -0.6245 \end{bmatrix}$	$\begin{bmatrix} 0\angle 0 \\ 0.0341\angle 0.0341 \\ 0.0341\angle 0.0341 \\ 0\angle 0 \end{bmatrix}^T$

TABLE V
Controller Gains for Fault-Free and Reconfigurable Control

Cases	Feedback controller gains	Feedforward gains
Fault-free	$\begin{bmatrix} 0.7074 & -0.1382 & -0.7454 & -1.0289 \\ 0.1149 & -0.5734 & 0.0224 & 0.4577 \end{bmatrix}$	$\begin{bmatrix} 0.7746 & -0.1460 \\ 0.1434 & -0.7285 \end{bmatrix}$
System fault	$\begin{bmatrix} 0.5558 & 1.3050 & -0.7765 & -0.8605 \\ 0.1863 & 1.2946 & -0.0854 & 0.3494 \end{bmatrix}$	$\begin{bmatrix} 0.6192 & 1.4052 \\ 0.2173 & -0.3845 \end{bmatrix}$
Actuator fault	$\begin{bmatrix} 2.0084 & 0.4717 & -2.0855 & -3.1088 \\ -0.3869 & -1.0500 & 0.6298 & 1.5973 \end{bmatrix}$	$\begin{bmatrix} 2.2253 & 0.4918 \\ -0.3981 & -1.3067 \end{bmatrix}$
Sensor fault	$\begin{bmatrix} 0.7074 & -0.1382 & -0.7454 & -1.0289 \\ 0.1149 & -0.5734 & 0.0224 & 0.4577 \end{bmatrix}$	$\begin{bmatrix} 0.7746 & -0.1460 \\ 0.1434 & -0.7285 \end{bmatrix}$

eigenvectors are to those of the prefault system, misalignment of the eigenvectors are calculated in terms of distances and angles between them which are shown in Table IV.

As can be seen from the Table IV, the new eigenvectors are very close to those of the prefault system.

2) *Responses of the System Under Component Failure*: The plant and reconfigured output responses in the presence of the system component faults are illustrated in Fig. 4. For comparison purpose, the plant output responses without the controller reconfiguration are also shown. It can be seen that the output responses of the fault-free closed-loop system is recovered by using the proposed approach after a short transient. However, without the controller reconfiguration, the system becomes unstable. The mode probability and the control switching sequence for FDD and the controller reconfiguration are shown in Fig. 5. It can be observed that even though there are a few mis-switchings at the beginning stage of the reconfiguration (around $t = 5$ s), satisfactory performance has eventually been achieved. Fig. 6 demonstrates the closed-loop control signals in the two control channels, from which one can easily examine how the closed-loop control signals have been adjusted accordingly to compensate for the fault.

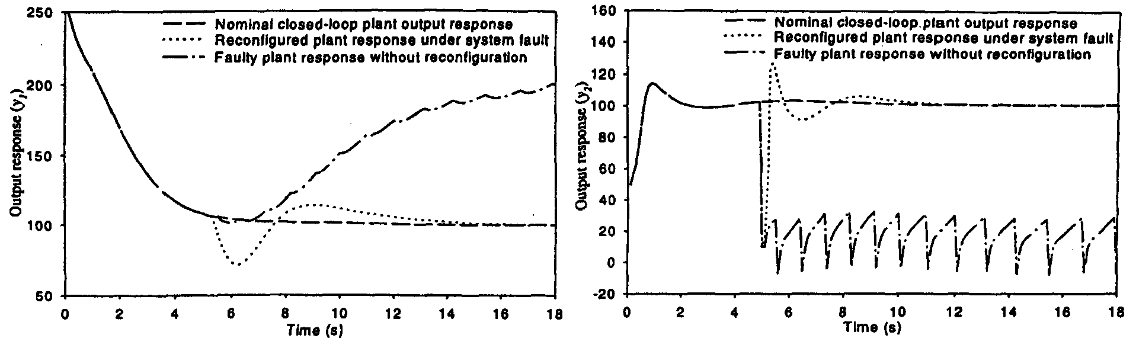

Fig. 4. Output responses under system component fault.

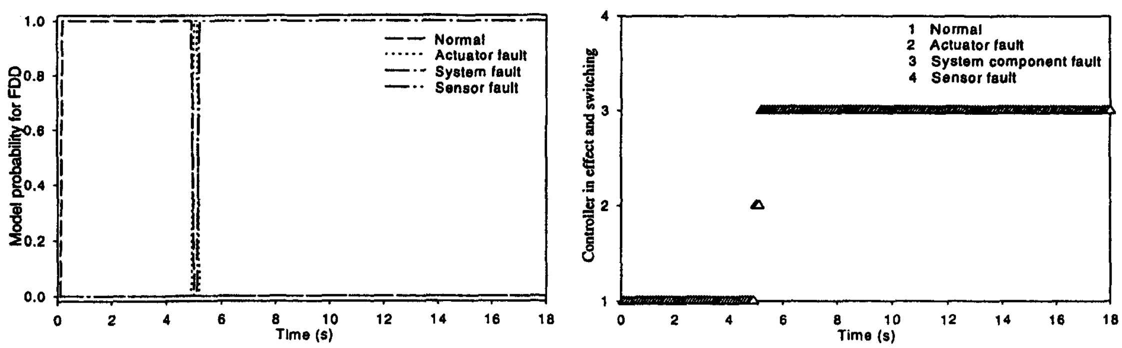

Fig. 5. Mode probability and control switching sequence under system component fault.

TABLE VI
Performance of Proposed Scheme

Faults	Performance of FDD						Performance of reconfiguration				
	CDI	FA	IFI	MD	NMD	DCID	CR	IR	RD	$\bar{e}$	e_{max}
system	98.88%	0%	1.12%	0%	0%	0.2s	98.88%	1.12%	0.2s	6.969	92.40
actuator	99.64%	0.01%	0%	0.13%	0.22%	0.06s	99.69%	0.31%	0.06s	1.068	6.450
sensor	100.0%	0%	0%	0%	0%	0s	100.0%	0%	0s	0.313	0.603

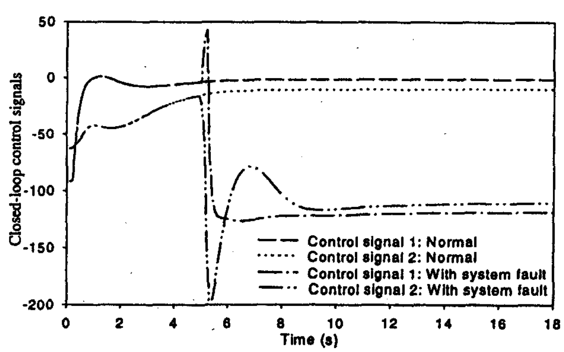

Fig. 6. Closed-loop controller output under system component fault.

In addition, the quantitative performance indices described previously are given in Table VI. Table VII presents the results for the case with perfect FDD for reconfiguration. All results in the Tables VI and VII are the average of 100 Monte Carlo simulation runs. Compared with the performance with correct (perfect) FDD and reconfiguration, satisfactory performance has been obtained via the proposed integrated active fault-tolerant control scheme.

3) *Responses of the System Under Actuator Failure*: The plant and reconfigured output responses in the presence of the actuator fault are illustrated in Fig. 7. It can be seen that the output responses of the original closed-loop system are completely recovered. The corresponding mode probability and the control switching sequence are given in Fig. 8. However, without the controller reconfiguration, the closed-loop system becomes unstable. Fig. 9 demonstrates the corresponding control signals. Similar to the case of the system component fault, performance indices are also given in Tables VI and VII.

4) *Responses of the System Under Sensor Failure*: Figs. 10–12 show the behavior of the system in the presence of the sensor fault. Satisfactory FDD and reconfiguration results have been obtained. It should be noted that even though the design of the

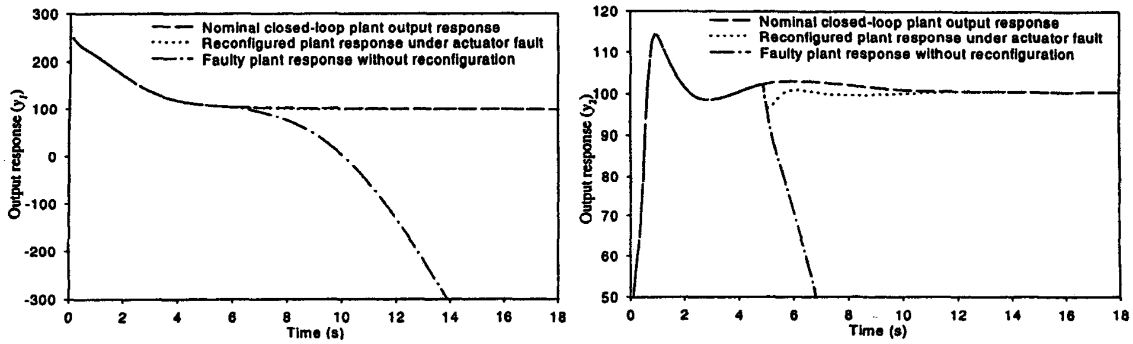

Fig. 7. Output responses under actuator fault.

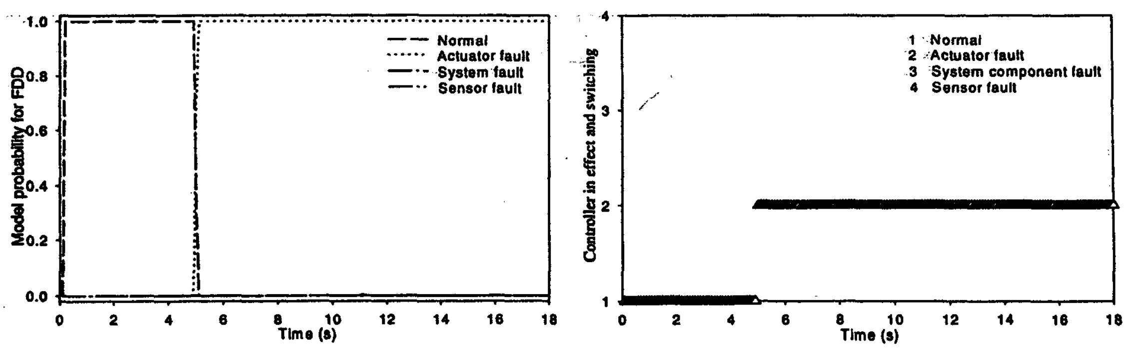

Fig. 8. Mode probability and control switching sequence under actuator fault.

TABLE VII
Performance of FDD and FTCS with Correct FDD and Reconfiguration

Faults	Performance of FDD						Performance of reconfiguration			
	CDI	FA	IFI	MD	NMD	DCID	CR	IR	$\bar{e}$	e_{max}
system	100%	0%	0%	0%	0%	0s	100%	0%	8.633	92.40
actuator	100%	0%	0%	0%	0%	0s	100%	0%	1.091	5.354
sensor	100%	0%	0%	0%	0%	0s	100%	0%	0.313	0.603

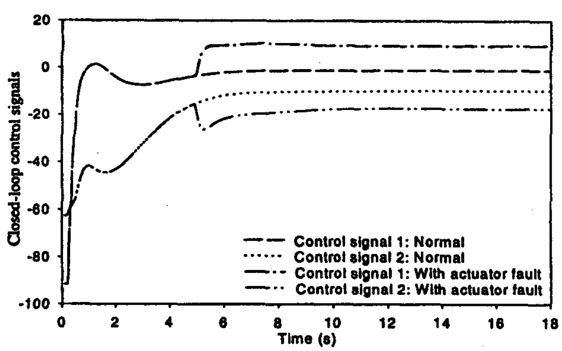

Fig. 9. Closed-loop control input under actuator fault.

reconfigurable feedback controller is not influenced directly by sensor faults due to the feedback of the estimated states, sensor faults do affect the implementation of the closed-loop control. This can be observed from Fig. 11. Fig. 12 demonstrates the control signals in the presence of the sensor fault. Due to the fact that the same control law has been used as the normal controller, and that the satisfactory state estimation for both fault-free and fault cases have been obtained. There are no obvious changes in the corresponding closed-loop control signals. This fact can also be seen from Tables VI and VII.

The results from the simulation have indicated that the proposed integrated FDD and reconfigurable control scheme can deal with system component, actuator and sensor faults effectively.

VI. CONCLUSIONS

An integrated MM fault detection, diagnosis, and reconfigurable control scheme has been proposed. FDD has been carried out using the IMM approach. Steady-state tracking of a constant reference command has been achieved using a feedforward control technique, and the reconfigurable controller is

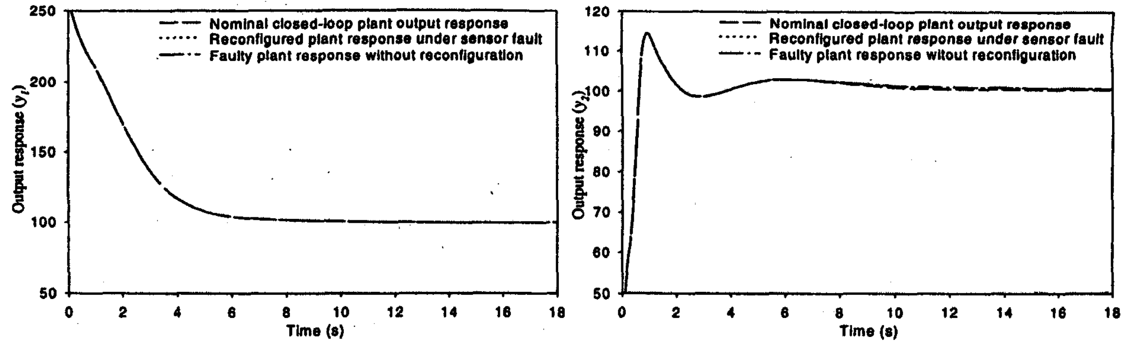

Fig. 10. Output responses under sensor fault.

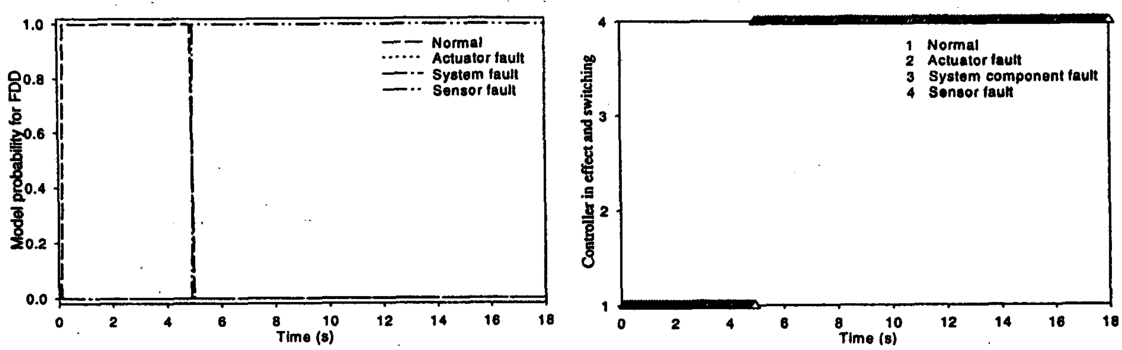

Fig. 11. Mode probability and control switching sequence under sensor fault.

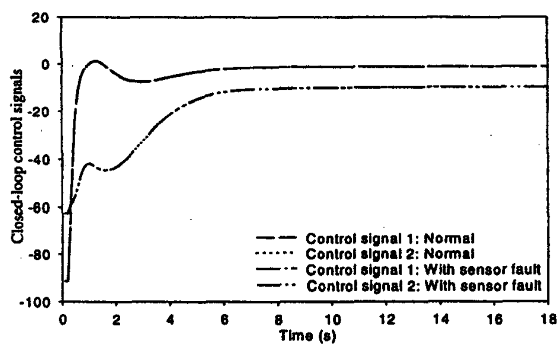

Fig. 12. Closed-loop control input under sensor fault.

designed via eigenstructure assignment. To achieve fast and reliable fault detection, diagnosis, and controller reconfiguration, an index related to the closed-loop performance has been combined with the information of the mode probability. New strategy for generation of the aggregated reconfigurable control signal has also been proposed. Several performance indices have been introduced for the evaluation of the integrated FDD and reconfigurable control scheme. Simulation results for an aircraft example in the presence of system component, actuator and sensor faults have shown the effectiveness of the proposed approach.

REFERENCES

[1] Andry, A. N., Jr., Sharipo, E. Y., and Chung, J. C. (1983)
Eigenstructure assignment for linear systems.
IEEE Transactions on Aerospace and Electronic Systems, **19** (Sept. 1983), 711–729.

[2] Athans, M., Castanon, D., Dunn, K., Greene, C. S., Lee, W. H., Sandell, N. R., Jr., and Willsky, A. S. (1977)
The stochastic control of the F-8C aircraft using a multiple model adaptive control (MMAC) method—Part 1: Equilibrium flight.
IEEE Transactions on Automatic Control, **22** (May 1977), 768–780.

[3] Balle, P., Fischera, M., Fussel, D., Nells, O., and Isermann, R. (1998)
Integrated control, diagnosis and reconfiguration of a heat exchanger.
IEEE Control Systems (June 1998), 52–63.

[4] Basseville, M. (1988)
Detecting changes in signals and systems—A survey.
Automatica, **24** (1988), 309–326.

[5] Blom, H. A. P., and Bar-Shalom, Y. (1988)
The interacting multiple model algorithm for systems with Markovian switching coefficients.
IEEE Transactions on Automatic Control, **33** (Aug. 1988), 780–783.

[6] Bodson, M., and Groszkiewicz, J. (1997)
Multivariable adaptive algorithms for reconfigurable flight control.
IEEE Transactions on Control System Technology, **5** (Mar. 1997), 217–229.

[7] Boskovic, J., and Mehra, R. K. (1998)
A multiple model-based reconfigurable flight control system design.
In *Proceedings of the 37th IEEE Conference on Decision and Control*, Tampa, FL, Dec. 1998, 4503–4508.

[8] Chandler, P. R. (1984)
Self-repairing flight control system reliability and maintainability program executive overview.
In *Proceedings of the IEEE National Aerospace and Electronics Conference*, Dayton, OH, 1984, 586–590.

[9] Chen, J., and Patton, R. J. (1999)
Robust Model-based Fault Diagnosis for Dynamic Systems.
Norwell, MS: Kluwer Academic Publishers, 1999.

[10] Frank, P. M. (1990)
Fault diagnosis in dynamic systems using analytical and knowledge-based redundancy—A survey and some new results.
Automatica, **26** (1990), 459–474.

[11] Gao, Z., and Antsaklis, P. J. (1991)
Stability of the pseudo-inverse method for reconfigurable control systems.
International Journal of Control, **53** (1991), 717–729.

[12] Huang, C. Y., and Stengel, R. F. (1990)
Restructurable control using proportional-integral implicit model following.
Journal of Guidance, Control, and Dynamics, **13** (Mar.–Apr. 1990), 303–309.

[13] Jiang, J. (1994)
Design of reconfigurable control systems using eigenstructure assignment.
International Journal of Control, **59** (1994), 395–410.

[14] Jiang, J., and Zhao, Q. (1998)
Fault tolerant contol system synthesis using imprecise fault identification and reconfiguration control.
In *Proceedings of the IEEE International Symposium on Intelligent Control*, Gaithersburg, MD, Sept. 1998, 169–174.

[15] Jiang, J., and Zhao, Q. (2000)
Design of reliable control systems possessing actuator redundancies.
Journal of Guidance, Control, and Dynamics, **23** (July–Aug. 2000), 709–718.

[16] Li, X. R. (1996)
Hybrid estimation techniques.
In C. T. Leondes (Ed.), *Control and Dynamic Systems*, **76**.
New York: Academic Press, 1996, 213–287.

[17] Looze, D. P., Weiss, J. L., Eterno, J. S., and Barrett, N. M. (1985)
An automatic redesign approach for restructurable control systems.
IEEE Control System Magazine (May 1985), 16–22.

[18] Maybeck, P. S., and Hanlon, P. D. (1995)
Performance enhancement of a multiple model adaptive estimator.
IEEE Transactions on Aerospace and Electronic Systems, **31** (Oct. 1995), 1240–1254.

[19] Maybeck, P. S., and Stevens, R. D. (1991)
Reconfigurable flight control via multiple model adaptive control methods.
IEEE Transactions on Aerospace and Electronic Systems, **27** (May 1991), 470–479.

[20] Mazor, E., Averbuch, A., and Bar-Shalom, Y. (1998)
Interacting multiple model methods in target tracking: A survey.
IEEE Transactions on Aerospace and Electronic Systems, **34** (Jan. 1998), 103–123.

[21] Moerder, D. D., Halyo, N., Broussard, J. R., and Caglayan, A. K. (1989)
Application of precomputed control laws in a reconfigurable aircraft flight control system.
Journal of Guidance, Control, and Dynamics, **12** (May–June 1989), 325–333.

[22] Morse, W. D., and Ossman, K. A. (1990)
Model following reconfigurable flight control systems for the AFTI/F-16.
Journal of Guidance, Control, and Dynamics, **13** (Nov.–Dec. 1990), 969–976.

[23] Napolitano, M. R., Naylor, S., Neppach, C., and Casdorph, V. (1995)
On-line learning nonlinear direct neurocontrollers for restructurable control systems.
Journal of Guidance, Control, and Dynamics, **18** (Jan.–Feb. 1995), 170–176.

[24] Napolitano, M. R., and Swaim, R. L. (1991)
New technique for aircraft flight control reconfiguration.
Journal of Guidance, Control, and Dynamics, **14** (Jan.–Feb. 1991), 184–190.

[25] Narendra, K. S. Balakrishnan, J., and Coliz, M. K. (1995)
Adaptation and learning using multiple models, switching, and tuning.
IEEE Control System Magazine (June 1995), 37–51.

[26] Narendra, K. S., and Tripathi, S. S. (1973)
Identification and optimization of aircraft dynamics.
Journal of Aircraft, **10** (Jan. 1973), 193–199.

[27] Noura, H., Sauter, D., Hamelin, F., and Theilliol, D. (2000)
Fault-tolerant control in dynamic systems: Application to a winding machine.
IEEE Control System Magazine (Feb. 2000), 33–49.

[28] Patton, R. J. (1997)
Fault-tolerant control: The 1997 situation.
In *Proceedings of IFAC Symposium SAFEPROCESS'97*, Hull, UK, Aug. 1997, 1033–1055.

[29] Patton, R. J., Frank, P. M., and Clark, R. N. (1989)
Fault Diagnosis in Dynamic Systems, Theory and Applications.
Englewood Cliffs, NJ: Prentice-Hall, 1989.

[30] Rago, C., Prasanth, R., Mehra, R. K., and Fortenbaugh, R. (1998)
Failure detection and identification and fault tolerant control using the IMM-KF with applications to the eagle-eye UAV.
In *Proceedings of the 37th IEEE Conference on Decision and Control*, Tampa, FA, Dec. 1998, 4208–4213.

[31] Rauch, H. E. (1995)
Autonomous control reconfiguration.
IEEE Control System Magazine (Dec. 1995), 37–48.

[32] Schott, K. D., and Bequette, B. W. (1997)
Multiple model adaptive control.
In R. Murray-Smith and T. A. Johansen (Eds.), *Multiple Model Approaches to Modeling and Control.*
London, UK: Taylor and Francis, 1997, 269–291.

[33] Veillette, R. J., Medanic, J. V., and Perkins, W. R. (1992)
Design of reliable control systems.
IEEE Transactions on Automatic Control, **37** (Mar. 1992), 290–300.

[34] Willsky, A. S. (1976)
A survey of design methods for failure detection in dynamic systems.
Automatica, **12** (1976), 601–611.

[35] Zhang, Y. M., and Jiang, J. (2001)
Integrated design of reconfigurable fault-tolerant control systems.
Journal of Guidance, Control, and Dynamics, **24** (Jan.–Feb. 2001), 133–136.

[36] Zhang, Y. M., and Li, X. R. (1998)
Detection and diagnosis of sensor and actuator failures using IMM estimator.
IEEE Transactions on Aerospace and Electronic Systems, **34** (Oct. 1998), 1293–1313.

[37] Zhou, D. H., and Frank, P. M. (1998)
Fault diagnosis and fault tolerant control.
IEEE Transactions on Aerospace and Electronic Systems, **34** (Apr. 1998), 420–427.

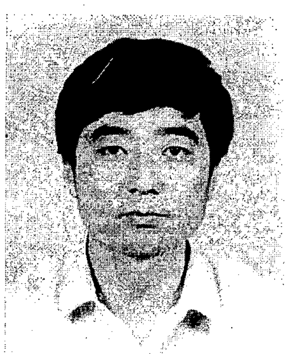

Youmin Zhang (M'99) received the B.S., M.S. and Ph.D. degrees in electrical engineering from Northwestern Polytechnical University, Xian, P. R. China, in 1983, 1986, and 1995, respectively.

Since 1986, he has worked in the Department of Automatic Control, Northwestern Polytechnical University, Xian, P. R. China, where he was promoted as an Associate Professor in 1992 and was appointed as an Associate Chair of the Department in 1994. During Sept. 1995 and Aug. 2000, he held several research positions in the University of New Orleans, Louisiana State University, State University of New York at Binghamton, and The University of Western Ontario, respectively. He is currently an Assistant Professor in the Department of Electrical and Computer Engineering at The University of Western Ontario, London, Ontario, Canada. His main research interests include fault detection, diagnosis and fault-tolerant (control) systems; machinery condition monitoring; signal and data processing; estimation, identification theory and algorithms for signal processing, communications, and control; neural networks and applications to modeling, identification, diagnosis and control.

Dr. Zhang has published 34 refereed journal papers and more than 50 international conference papers, edited one monograph and coauthored a graduate textbook. He received an award from Natural Sciences and Engineering Research Council (NSERC) of Canada for a Visiting Fellowship in Canadian Government Laboratories. He was the recipient of several research achievement awards from National Education Commission of China, Aeronautics and Astronauts Industry Ministry of China, and Shaanxi Province Education Commission; an outstanding teaching achievement award from Shaanxi Province; several outstanding teaching and research awards from Northwestern Polytechnical University. He served as the General Chair of the 10th Youth Conference on Automatic Control and Automation in China in 1994 and an international program committee member of several international conferences. He served as an Associate Editor of the 2001 IEEE Conference on Control Applications. He serves also as a reviewer of several refereed international journals and conferences.

Jin Jiang (M'85—SM'94) obtained his Ph.D. in electrical engineering from the University of New Brunswick, Fredericton, New Brunswick, Canada, in 1989.

Currently, he is a Professor in the Department of Electrical and Computer Engineering at The University of Western Ontario, London, Ontario, Canada. His research interests are in the areas of fault-tolerant control of safety-critical systems, power system dynamics and controls, and advanced signal processing.